JOURNAL OF GEOPHYSICAL RESEARCH, VOL. 106, NO. A9, PAGES 18,495–18,504, SEPTEMBER 1, 2001

Nonlinear response of the polar ionosphere to large values of the interplanetary electric field

C. T. Russell

Institute of Geophysics and Planetary Physics, University of California, Los Angeles, California

J. G. Luhmann

Space Sciences Laboratory, University of California, Berkeley, California

G. Lu

High-Altitude Observatory, National Center for Atmospheric Research, Boulder, Colorado

Abstract. During large geomagnetic storms the polar cap potential drop fluctuates, but its average value seldom reaches 150 kV and its peak value seldom reaches 200 kV. Since the quiet time potential drop is about 40 kV and since the interplanetary electric field (IEF) is greatly enhanced during storms, this relative constancy appears to be due to a saturation effect. This apparent saturation phenomenon has been previously noted but has not received much attention in the recent literature, in spite of its importance during magnetic storms and in spite of the fact that it seems not to be understood. The IEF and the polar cap potential drop appear to have a very linear relationship up to about 80 kV. At greater IEF the potential drop increases only slightly. We use the assimilative mapping of ionospheric electrodynamics procedure to illustrate this saturation on a case-by-case basis during a number of recent storms. We confirm using DE 2 data that the saturation of the potential drop is a real effect and is not an artifact of the measurement process. Observations of the plasmapause and the buildup of the ring current indicate a linear response to the IEF over a wide range of solar wind conditions. Thus the convection of the magnetospheric plasma and the injection of energy into the ring current seem not to be affected by this saturation.

1. Introduction

Conventional wisdom treats the polar cap as a resistor across which the interplanetary electric field applies a voltage. The voltage drop is controlled by the rate of reconnection and is a direct measure of this rate, being the voltage drop integrated along the neutral line. This is popularly called the voltage generator model of the solar wind interaction. Taken literally, the voltage drop across the polar cap should then equal the interplanetary electric field (IEF) across the streamlines mapped back into the solar wind from the two opposite ends of the neutral line. Empirically, we know that subsolar reconnection, that transfers magnetic flux from the dayside magnetosphere into the tail, does not occur for the northward interplanetary magnetic field (IMF), that is, dusk-to-dawn IEF [e.g., *Scurry and Russell*, 1991]. Thus we calculate this electric field from the southward interplanetary magnetic field, letting northward fields equal zero. If the length of the reconnection line on the magnetopause were determined just by geometry and were constant, so that it always mapped back to the same length in the solar wind, then we might expect that the reconnection rate would be proportional to the IEF. However, we do not know a priori what controls the size of reconnection region and therefore the rate of reconnection. *Burton et al.* [1975] empirically determined the reconnection rate dependence by examining the rate of energization of the ring current during the main phase of geomagnetic storms. They found a linear dependence for all sized storms, once a threshold of 0.5 mV m^{-1} was passed.

Earlier investigations of the potential drop across the polar cap suggested that for large southward interplanetary magnetic fields the relationship between the polar cap potential drop and the interplanetary electric field seemed to saturate [e.g., *Reiff and Luhmann*, 1986]. Some recent analyses based on a large set of DMSP data, on the other hand, found no evidence of such saturation [*Boyle et al.*, 1997]. However, their polar cap potential drops are for the most part below 100 kV and they did not

Table 1. Input Parameters to the AMIE procedure

Storm	Number of Magneto-meters[a]	DMSP Satellites Particles	DMSP Satellites Ion Drift	NOAA Satellites	Super DARN HF Radars
January 1997	82	3	3	2	6
May 1998	88	4	0	2	6
September 1998	86	4	2	2	6
October 1995	77	2	2	2	5
October 1998	92	4	1	2	0

[a]In Northern Hemisphere above 50° magnetic latitude.

Paper number 2001JA900053.
0148-0227/01/2001JA900053$09.00

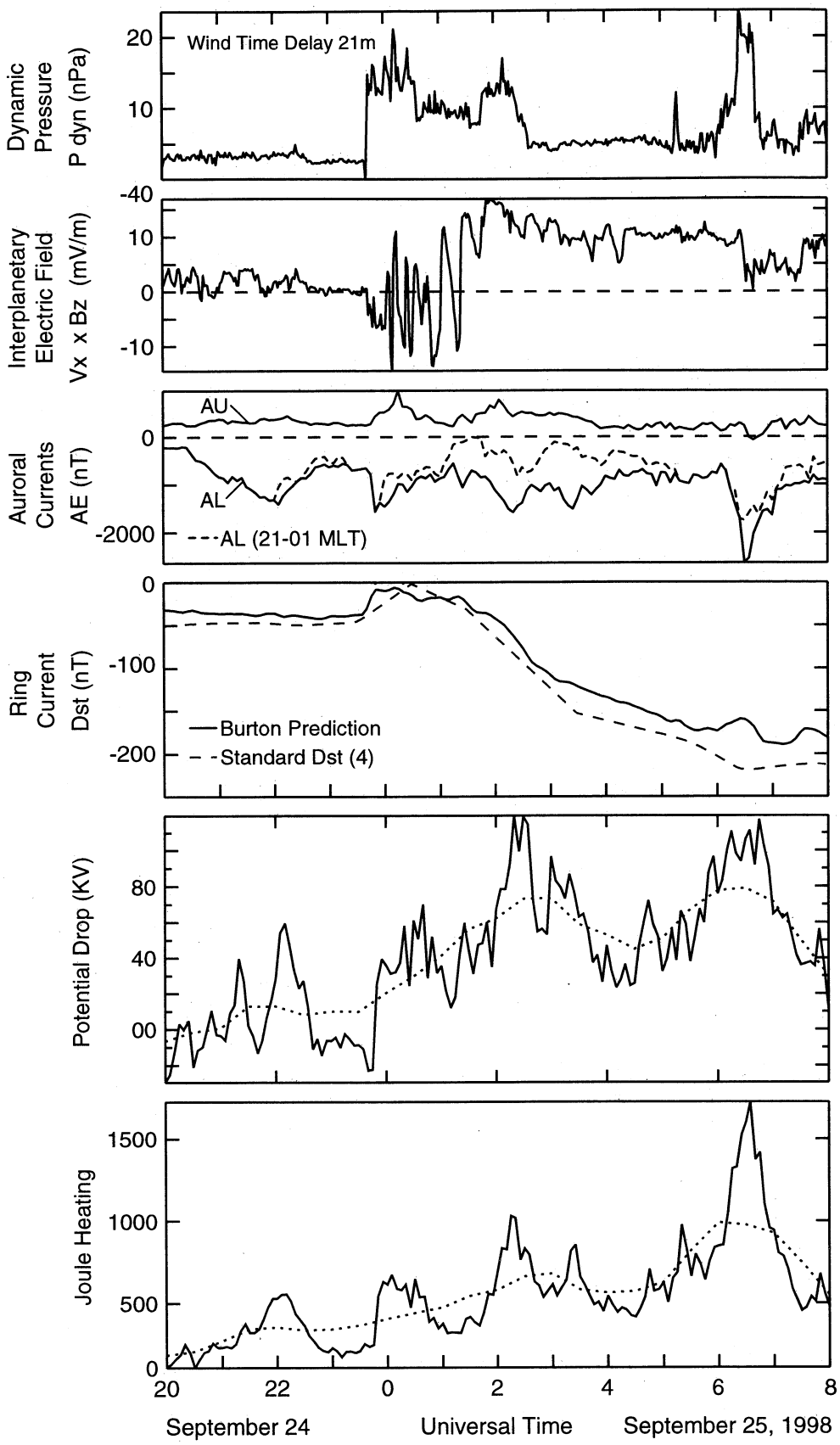

Figure 1. Geomagnetic storm of September 24-25, 1998. (top to bottom) The interplanetary electric field, the *AE* index, the *Dst* index, the potential drop across the polar cap, and the Joule heating in the auroral regions from the AMIE model.

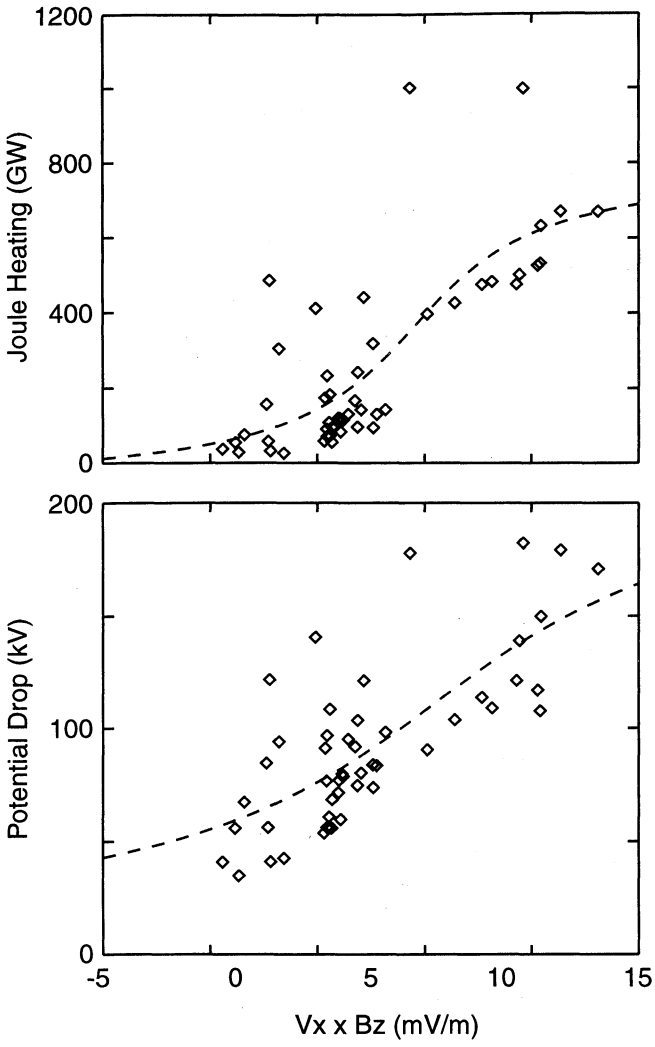

Figure 2. One hour averages of the potential drop across the polar cap and the Joule heating versus the IEF with arctan fit during the September 24-25, 1998, storm.

correlate with the interplanetary electric field only with the magnetic field. Here we use a sample set of magnetic storm periods, when large southward interplanetary magnetic fields, and thus electric fields, are present, to demonstrate that the saturation effect is real and comes into play during significant storms. Our motivation is to resurrect this problem and document it with a modern set of data because the polar ionospheric response is a key element of the space weather of the magnetosphere/ ionosphere system.

MHD simulations suggest [*Fedder and Lyon*, 1987] that the polar cap electrical conductivity controls in part the reconnection rate. One could imagine that a highly electrically conducting polar cap could freeze convection and the magnetic flux, opened by reconnection, would pile up in the magnetotail. Eventually, this would become such a large obstacle to the flow that the tail would deflect the solar wind and no more reconnection would take place. Alternatively, if the polar cap conductivity limited the rate of reconnection at the magnetopause, a magnetic barrier would build up in the magnetosheath and the flow would be deflected around the magnetosphere.

What really does happen? We can further constrain the answer in two ways. We can infer the potential drop from the assimilative mapping of ionospheric electrodynamics (AMIE) procedure [*Richmond and Kamide*, 1988], and we can examine electric field measurements across the polar cap. We use AMIE results for five storms: September 24-25, 1998; May 2-5, 1998; January 9-11, 1997; October 18-20, 1995; and October 18-20, 1998. The measured potential drops will be taken from the statistical study of DE 2 data by *Weimer* [1995] as reanalyzed by *Burke et al.* [1999]. Having confirmed the existence of the saturation effect during these storms, we suggest further analyses that may lead to better understanding of the underlying physical cause.

2. Observations

The observed magnetospheric response for the five storms we investigate will be summarized by the outputs of the AMIE procedure [*Richmond and Kamide*, 1988]. As part of the AMIE process we calculate the polar cap potential drop and the Joule dissipation. Using the large number of stations that contribute to the AMIE analysis, we separately calculate an improved AE and *Dst* index. For each of the storms we display first the time series of the solar wind and magnetospheric parameters and then in a separate figure the Joule heating and the potential drop versus the IEF. The IEF is taken to be the solar wind velocity times the north-south component of the IMF in solar magnetospheric coordinates. A positive value of the IEF is from dawn to dusk and a negative value from dusk to dawn. We note that all main phases in our study begin with a sudden onset of a strong dawn-dusk electric field, because each of the causative interplanetary coronal mass ejections began with a strong southward IMF as expected for this period, the end of solar cycle 22 and the beginning of cycle 23 [cf. *Mulligan et al.*, 1998]. This behavior should change sometime in the current year (2000) because the strong leading field of the clouds should be northward. Table 1 lists the storms, the number of magnetometers used in the Northern Hemisphere above 50° magnetic latitude, the number of DMSP spacecraft contributing particle data and ion drift measurements, the number of NOAA satellites, and the number of high-frequency radars from the Super Dual Auroral Radar Network (SuperDARN) array used in the AMIE runs. The drift meters on the DMSP satellites are not used when the ion density is too low. NOAA satellites provide only electron energy flux and mean energy to the AMIE procedure. These are used to calculate Pedersen and Hall conductances. For the January 1997 storm the Polar ultraviolet imager (UVI) data also were used as input to the auroral conductance and to extract the auroral precipitation.

2.1. September 24-25, 1998

This period was active even before the interplanetary shock and magnetic cloud arrived. Figure 1 shows the solar wind dynamic pressure, electric field, the auroral zone currents, the *Dst*, predicted and observed, the polar cap potential drop and the Joule heating in the ionosphere. The auroral zone activity as measured by the *AE* index does not vary significantly throughout the period shown, even through the *Dst* index indicates a strong injection into the ring current in the middle of this figure. The potential drop and the Joule heating do rise but not as substantially as the ring current injection, nor are they phased with the ring current injection. In particular, the greatest Joule heating occurs when a density pulse is convected by the magnetosphere at 0630 UT while the ring current remains roughly constant.

The nonlinearity of the response of the potential and the Joule heating is illustrated more clearly in Figure 2 that shows 1

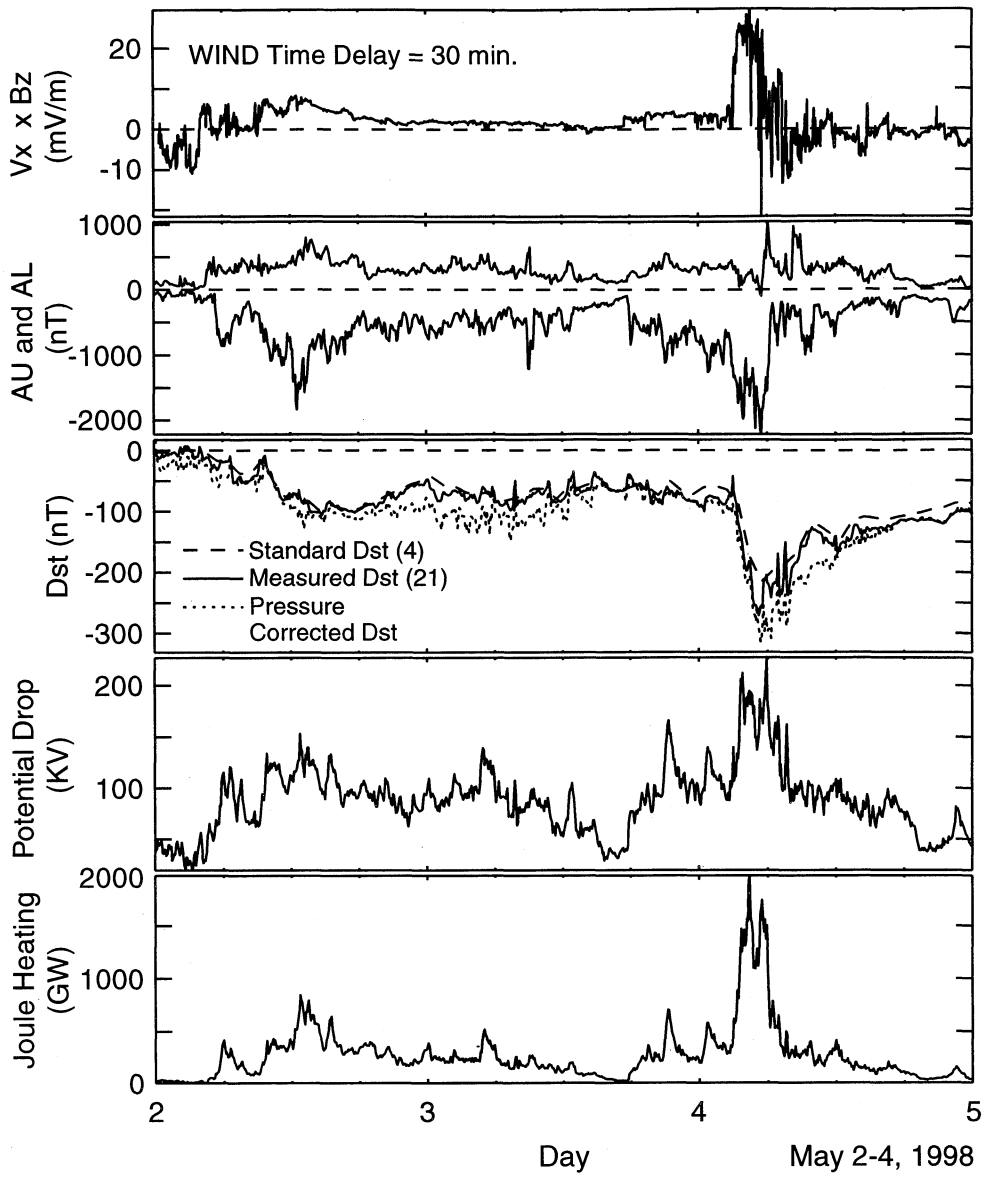

Figure 3. Geomagnetic storm of May 2-4, 1998. (top to bottom) The interplanetary electric field, the *AE* index, the *Dst* index, the potential drop across the polar cap, and the Joule heating in the auroral regions from the AMIE model.

the much greater interplanetary electric field, the potential drop reaches similar values in this storm as on the previous storm. The two largest heating periods do, but only slightly (15%), exceed the largest heating event of the previous storm despite the fact that the IEF is 70% larger. Figure 4 shows the plot of the Joule heating and potential drop versus IEF for this storm.

2.3. January 9-11, 1997

This well-studied storm began with an interplanetary magnetic field being horizontal and a more or less undisturbed magnetosphere. The observations are shown in Figure 5. After the arrival of the shock the IMF turns southward and both the auroral electrojet currents and the ring current build up. This apparent correlation between auroral currents and ring current injection is the basis for the frequent assertion that auroral zone activity can predict ring current injection despite the evidence seen in other storms such as September 24-25, 1998. In this storm the strongest Joule heating accompanies the ring current buildup but the largest potential drops do not. There are three hour averages plotted versus the IEF. There is much scatter due to the unsteady response of the magnetosphere to even steady input. There is also an apparent fly wheel effect in which, once a potential drop and Joule heating rate are established, they are maintained for a while when the IEF drops to low values or goes negative (dusk to dawn). The fly wheel effect causes the scatter on the left-hand side of the plot. In both top and bottom panels the polar cap responds rapidly to the IEF in the range 0 to 3 mV m^{-1}, reaching a potential drop and heating rate of about 120 kV and 500 GW at 3 mV m^{-1}. Then they increase only to about 180 kV and 700 GW at 10 mV m^{-1} and above with an occasional pulse of extra potential drop and Joule heating that appear to be temporal phenomena. It seems that above about 3 mV m^{-1} the response of the polar regions to the IEF undergoes a major change. In contrast, at lower latitudes the magnetospheric circulation pattern shows its expected sensitivity to the IEF on this day with erosion of the plasmasphere as low as L=2 [*Chi et al.*, 2000].

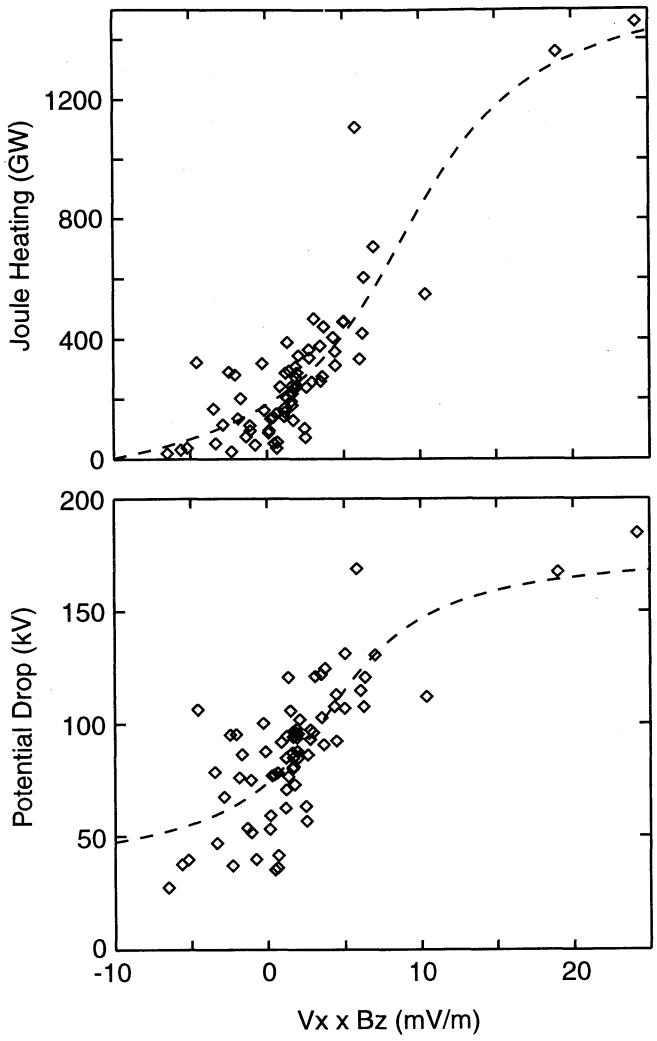

Figure 4. One hour averages of the potential drop across the polar cap and the Joule heating versus the IEF with arctan fit for the May 2-4, 1998, storm.

2.2. May 2-4, 1998

The most energetic recent storm was that of May 2-4, 1998. Again the magnetosphere was disturbed when the storm began. The observations on this day are shown in Figure 3 in a form similar to Figure 1. Despite the greater ring current injection and periods when the potential drop is about equal: during injection; near the beginning of the recovery phase; and during a weak injection into the ring current at midday on January 11. The correlations of Joule heating and potential drop with IEF are given in Figure 6. We note that this is a much smaller storm than the previous two storms, and the IEF reaches only about 7 mV m^{-1}. The potential drop reaches just over 100 kV and the maximum Joule heating is about 400 GW.

2.4. October 18-20, 1995

This storm is remarkably similar to the January 9-11, 1997, storm. The period shown in Figure 7 begins with a weak dawn-dusk IEF. It becomes fluctuating at the time of the interplanetary shock passage and then becomes strong and steady in the dawn-to-dusk direction triggering the development of the storm's main phase. The magnetic field direction rotates from southward to northward, and the IEF swings around to be dusk-to-dawn and the ring current recovers. Later there are a series of strong southward turnings that keep the ring current at a moderately disturbed level. In this storm, as in the January 1997 storm, the *AE* index and the Joule dissipation rise suddenly during the energization of the ring current, giving the appearance of a quantitative and perhaps causative correlation. Again and shown in Figure 8 the potential drop rises most rapidly versus the IEF near zero dawn-to-dusk IEF and appears to saturate.

2.5. October 18-20, 1998

This storm began with a sudden impulse when the IEF was weakly dawn to dusk and fluctuating. As illustrated in Figure 9 when the IEF became strong dawn to dusk at about 7 mV m^{-1} the ring current injection began and reached -125 nT. During the period of steady IEF the potential drop and the Joule heating were impulsive reaching about 200 kV and 800 GW, respectively, but averaging only 120 kT and 300 GW. Again as shown in Figure 10, the response of the polar cap is nonlinear or very slow.

3. Discussion

Despite the large scatter in the data due to the unsteadiness in both the IEF and the magnetospheric response, these five events imply that the polar cap potential drop, as deduced by the AMIE inversion, does not respond linearly with the IEF despite the evidence that the ring current injection and erosion of the plasmasphere appear to depend linearly on the IEF. One might then question if the AMIE model is correctly deducing the polar cap potential drop. However, this saturation is evident in previous case studies [e.g., *Ahn et al.*, 1992; *Cooper et al.*, 1995]. It is not peculiar to these storms. Despite the large increase in the IEF, the potential drop across the polar cap saturates in the region between 100 and 200 kV, and its temporal variation shows little correlation with the temporal variation of the IEF. For example, in the *Cooper et al.* [1995] study of the November 8, 1991, storm the potential drop maximizes at 213 kV.

This saturation is not due to the inability of the AMIE technique to sense large potential drops. The same behavior can be seen in Figure 11, after the statistical study of *Burke et al.* [1999], who compare DE 2 measurements of the polar cap potential drop with the IEF. We can use these statistical results to plot the polar cap potential drop versus IEF using the solar wind velocities given in the same paper, as shown in Figure 12. This potential drop is linear with the applied IEF up to about 3 mV m^{-1} and very insensitive to it above this level. We note that the potential drop plotted here is the difference between that found for due southward and northward IMF. This was not done for the events shown in Figures 1 to 10 or in the work of *Boyle et al.* [1997] accounting for the higher values of potential drop at saturation. We note that the Weimer-Burke potential drops saturate when the IEF reaches a value of about 3 mV m^{-1}. Our three storms had peak IEFs ranging from 7 to 24 mV m^{-1}, well into the nonlinear regime. Returning to the event studied by *Cooper et al.* [1995], for the solar wind conditions observed by IMP 8 on November 8, 1991, we would predict a potential drop of close to 600 kV using the linear portion of the relation in Figure 12 of this paper compared to the maximum of 213 kV seen. More recent studies also report evidence for saturation. *Ridley et al.* [1998] report that 11% of the events they examined showed an asymptotically changing potential drop. These authors noted that all the saturating changes were due to negative changes in IMF B_z but no values for B_z or the east-west component of the IEF were given for these events. Most recently, *Weimer* [2001]

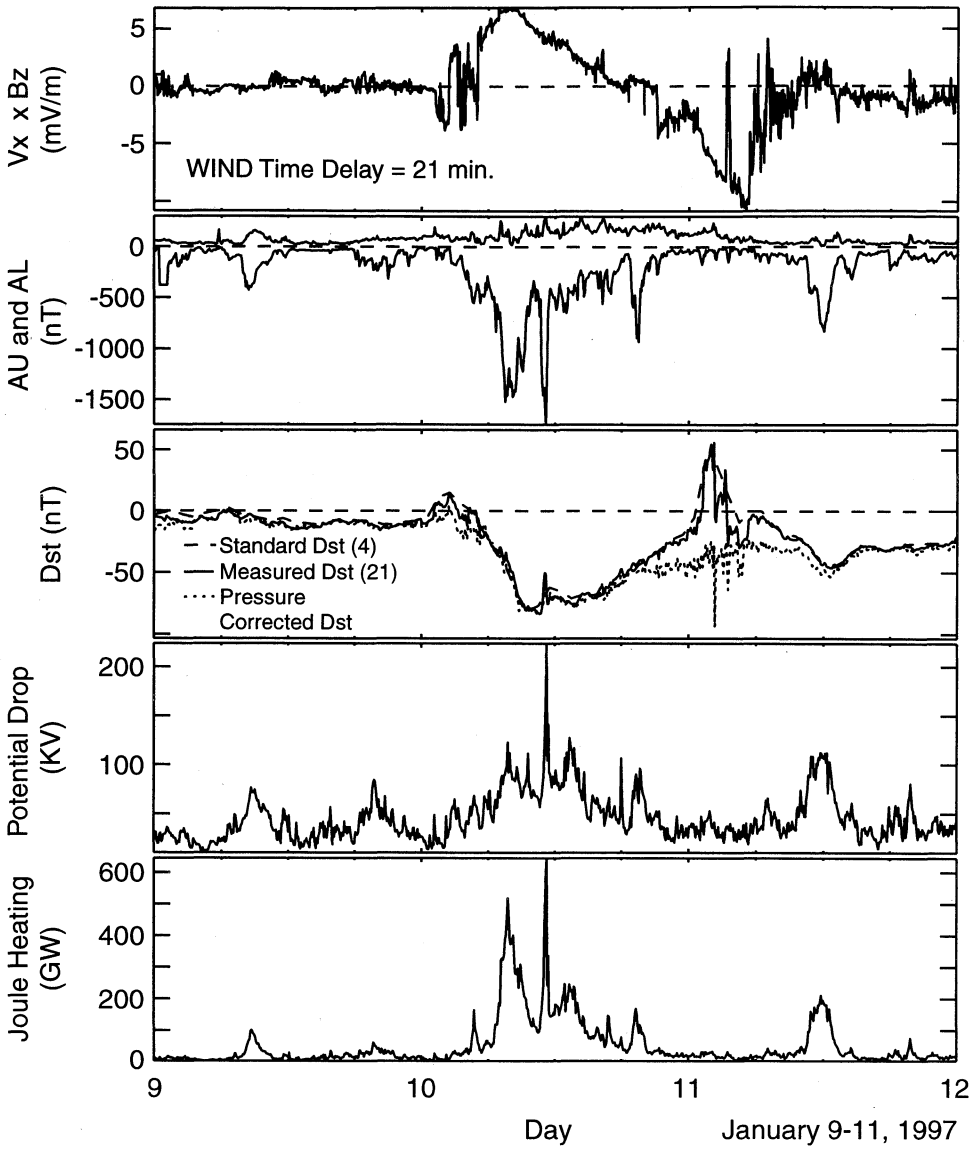

Figure 5. Geomagnetic storm of January 9-11, 1997. (top to bottom) The interplanetary electric field, the *AE* index, the *Dst* index, the potential drop across the polar cap, and the Joule heating in the auroral regions from the AMIE model.

shows a clear break in slope near 2.5 mV m^{-1} in his plot of polar cap potential drop versus IEF (top panel Figure 1). Not surprisingly this result is in agreement with the result in Figure 12 of this paper.

It would be least damaging to existing paradigms if this apparent saturation effect could be explained in terms of an artifact of the measurement process. It is difficult to find a single artifact that affects both. One physical process that could affect both is the rapid convection of slender flux tubes. AMIE, radars, and in situ drift measurement could all miss such "transient" features, but this would be a real effect, not an artifact of the measurement, and an important discovery for magnetospheric physics. Thus while we feel that it is important to reexamine carefully the measurement process, the measurements appear to be sufficiently accurate that we should consider what are their implications.

As mentioned above, one way to reduce the polar cap potential drop per unit of IEF is for the merging region on the nose of the magnetosphere to shrink for high values of the IEF. However, the ring current continues to build up during these storms, as one would expect from a linear dependence of the magnetospheric circulation on the IEF. Moreover, the plasmasphere was depleted down to at least L=2 during the September 24, 25 storm [*Chi et al.*, 2000]. This distance is close to the value expected for a 15 mV m^{-1} IEF if the efficiency of reconnection is of the order of 15-20%. This efficiency has to be significantly greater than the efficiency by which the magnetosphere taps into the solar wind energy flux because a large fraction of the energization of the magnetotail is immediately returned to the "solar wind" through the antisunward acceleration of plasma. It appears that the low-altitude polar cap ionosphere in which DE 2 is orbiting and to which AMIE is sensitive is not seeing the full potential drop in the high-altitude magnetosphere.

The need to accelerate low-altitude neutrals to the same speed as the ions is a possible cause of sluggishness in the response of polar cap convection; but, while the acceleration is occurring, the missing potential drop must appear somewhere else such as along magnetic field lines. It could also, for some time at

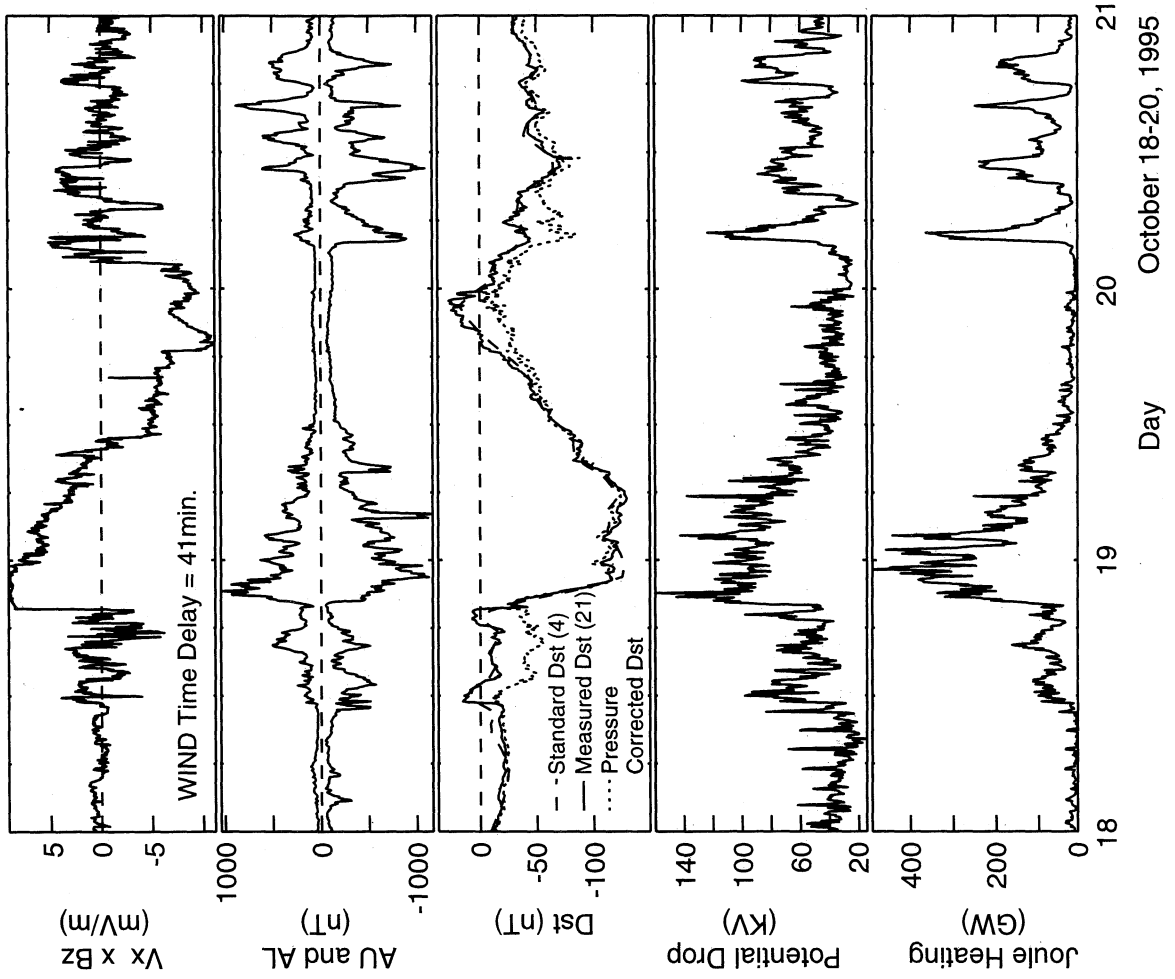

Figure 7. Geomagnetic storm of October 18-20, 1995. (top to bottom) The interplanetary electric field, the *AE* index, the *Dst* index, the potential drop across the polar cap, and the Joule heating in the auroral regions from the AMIE model.

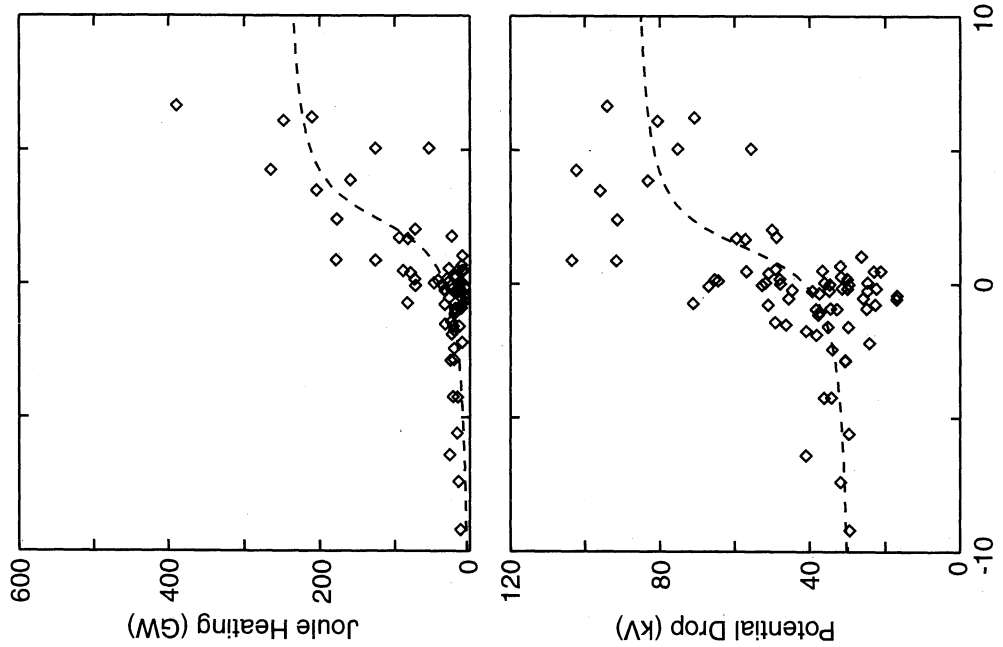

Figure 6. One hour averages of the potential drop across the polar cap and the Joule heating versus the IEF with arctan fit for the January 9-11, 1997, storm.

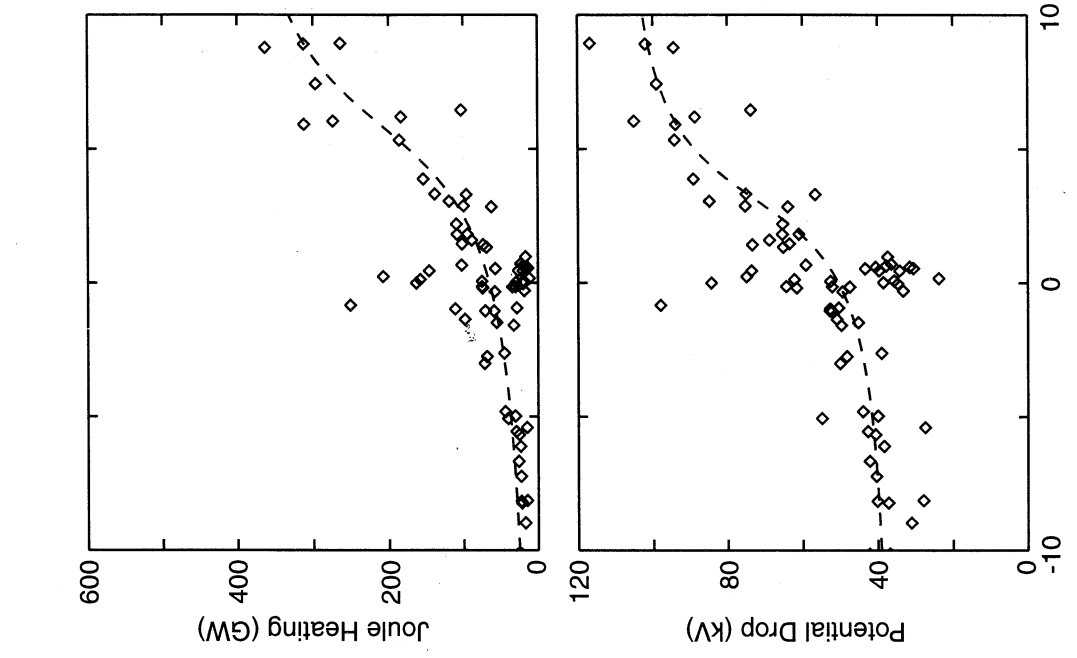

Figure 8. One hour averages of the potential drop across the polar cap and the Joule heating versus the IEF with arctan fit for the October 18-20, 1995, storm.

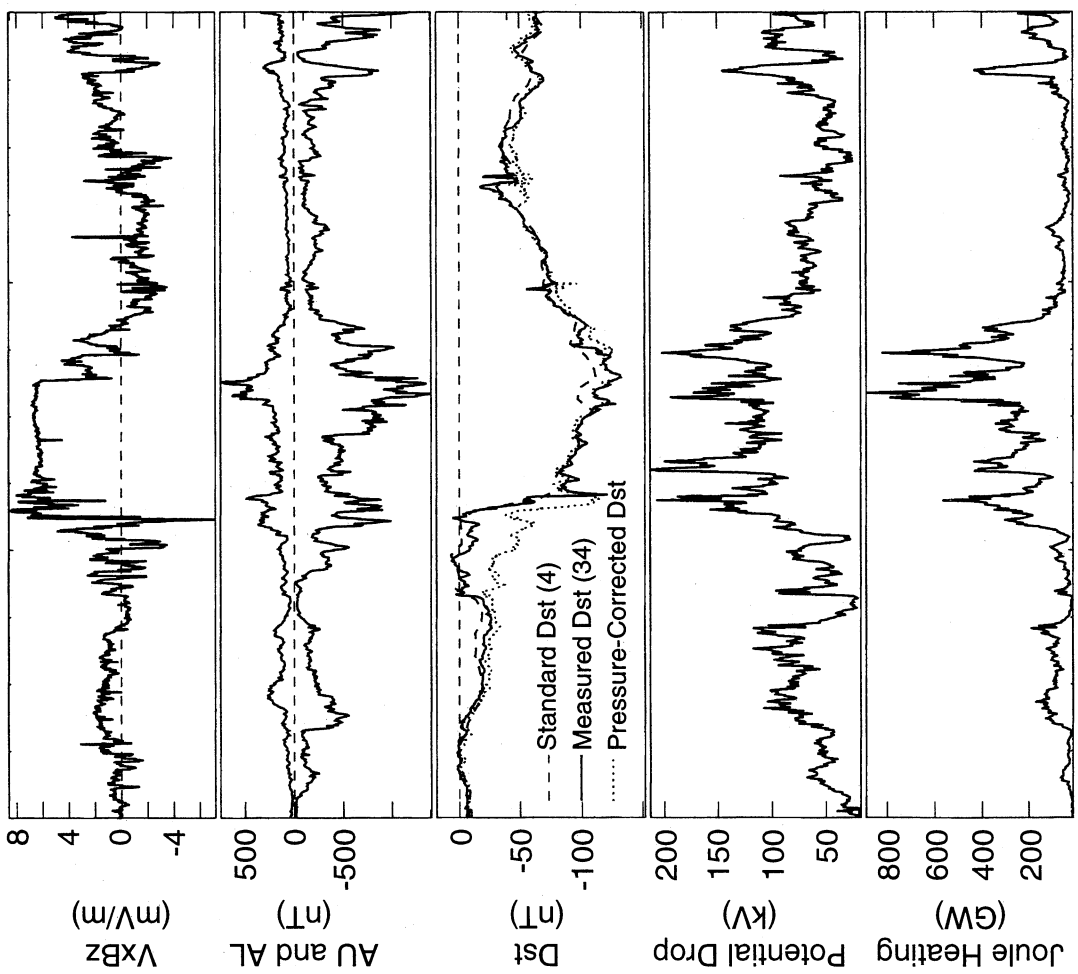

Figure 9. Geomagnetic storm of October 18-20, 1998. (top to bottom) The interplanetary electric field, the *AE* index, the *Dst* index, the potential drop across the polar cap, and the Joule heating in the auroral regions from the AMIE model.

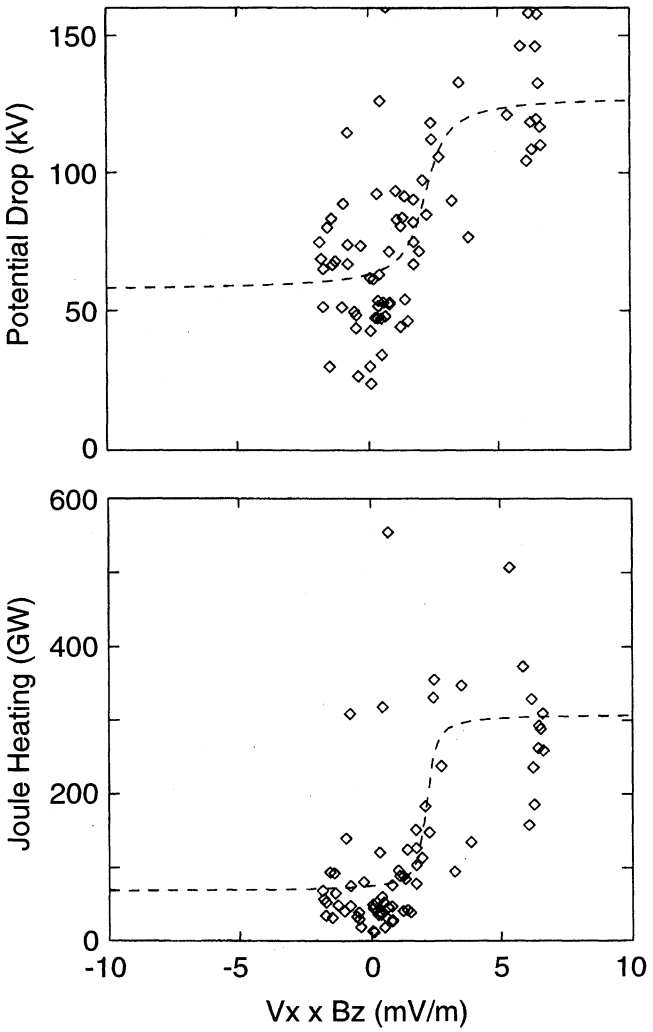

Figure 10. One hour averages of the potential drop across the polar cap and the Joule heating versus the IEF with arctan fit for the October 18-20, 1998, storm.

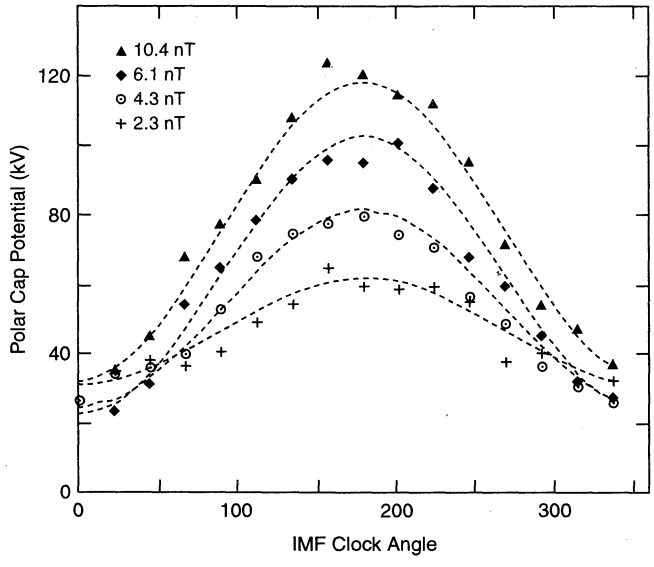

Figure 11. Observed potential drop across the polar cap from DE 2 measurements of *Weimer* [1995] as summarized versus IMF clock angle and IMF by *Burke et al.* [1999].

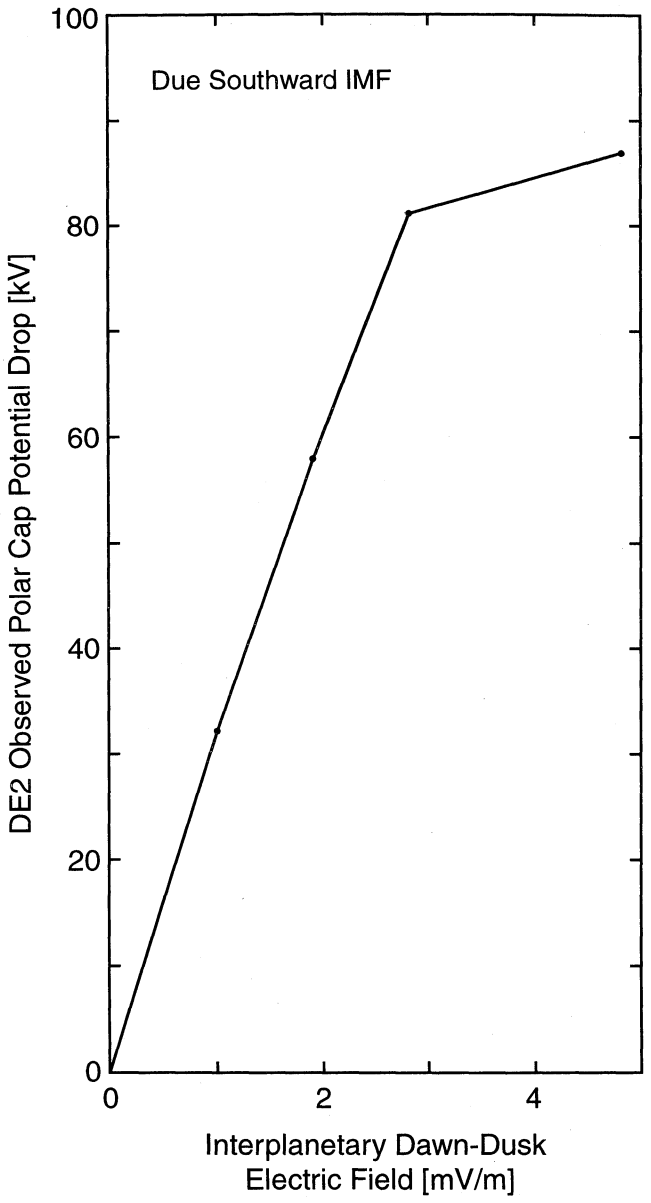

Figure 12. Potential drop plotted versus the corresponding value of the IEF for due southward IMF from the measurements in Figure 11.

least, appear as an inductive electric field associated with the growth of the flux content of the tail lobes. At low altitudes the feet of field lines frozen into the stationary polar ionosphere could join the polar cap without moving, by the simple act of changing their topology, while at high altitudes the flux was simultaneously being convected from the subsolar magnetopause into the tail.

AMIE and DE-2 differ from MHD models in estimating the polar cap potential drop. The MHD models are high by a factor of up to 2 [*Raeder et al.*, 1998]. The reasons for this could be one or more of the following: The MHD models ignore field-aligned potential drops; ionosphere conductivities in the MHD model are incorrect; or the region 2 currents are not properly treated in MHD models. The difference between MHD models and the observed potential drop is an important issue that also needs to be resolved but should not be confused with the nonlinearity discussed herein that is a pure observational effect and does not depend on the accuracy of MHD models. Nevertheless, MHD models can be an invaluable tool in understanding possible causes

of the potential drop saturation even if they imperfectly represent the magnetosphere. For example, the models can vary southward IMF and polar cap conductivity to test the linearity of the potential drop response.

Finally, we note the sluggishness of the Joule heating in its response to the IEF. The non-linearity seen in the potential drop response is less in the Joule heating, but the Joule heating, is clearly not directly linked to the IEF as the September 24-25, 1998, heating event at 0630 UT clearly shows. There may be an overall correlation during the storm between the IEF and the heating but individual peaks in heating do not have IEF counterparts.

A possibly important point for all these storms is that they began with a sudden onset of strong, steady southward IMF and a dawn-to-dusk electric field right after the passage of the magnetosheath plasma between the interplanetary shock and the leading edge of the interplanetary coronal mass ejection (ICME). As we noted above, this sequence is a direct consequence of the sign of the Sun's polar field that controls the leading polarity of flux ropes whose axes lie in the ecliptic plane. This field reverses every solar cycle just after solar maximum. Thus in the second half of the present solar cycle, similar ICMEs will cause an initial dusk-to-dawn IEF more slowly rotating to a dusk-to-dawn orientation, than the sudden onsets seen here. This could change the patterns seen in the potential drop versus IEF, as the magnetosphere will have a longer time to respond to the changed IEF and will not suddenly find itself responding to a strong reconnection rate.

4. Conclusions

During large geomagnetic storms the polar cap potential drop fluctuates but seldom exceeds 200 kV despite the existence of large values of the IEF. In examining the potential difference for due southward IMF referenced to that for due northward IMF, we find a linear dependence between the potential drop and the IEF over the range 0 to 3 mV m^{-1} which corresponds to a southward IMF of 7 nT for a median solar wind velocity of 440 km s^{-1}. The storms we examined had IEFs up to 24 mV m^{-1}. This lack of sensitivity of the polar cap to the IEF under large southward IMF conditions helps explain why the auroral zone currents are not good indicators of the development of large storms. The cold magnetospheric plasma in the plasmasphere and the hot plasma of the ring current seem strongly coupled to the IEF but the polar cap does not, except in a limited range for moderate storms. This problem of polar cap potential saturation is a key unsolved problem in magnetospheric physics that requires more work to resolve. While MHD models may be helpful in this regard, these models may need to include a parameterization of the field-aligned potential drop before they can do so.

Acknowledgments. The authors wish to thank D. R. Weimer for several helpful discussions of his measurements of the potential drop across the polar cap and the reality of the saturation effect. This work was supported by the National Aeronautics and Space Administration under grant NAG5-7721 and the National Science Foundation under grant ATM 98-03431.

Hiroshi Matsumoto thanks J. A. Fedder and another referee for their assistance in evaluating this paper.

References

Ahn, B.-H., Y. Kamide, K. W. Kroehl, and D. J. Gorney, Cross-polar cap potential difference, auroral electrojet indices and solar wind parameters, *J. Geophys. Res., 97*, 1345-1352, 1992.

Boyle, C. B., P. H. Reiff, and M. R. Hairston, Empirical polar cap potentials, *J. Geophys. Res., 102*, 111-125, 1997.

Burke, W. J., D. R. Weimer, and N. C. Maynard, Geoeffective interplanetary scale sizes derived from regression analysis of polar cap potentials, *J. Geophys. Res., 104*, 9989-9994, 1999.

Burton, R. K., R. L. McPherron, and C. T. Russell, An empirical relationship between interplanetary conditions and Dst, *J. Geophys. Res., 80*, 4204-4214, 1975.

Chi, P. J., C. T. Russell, S. Musman, W. K. Peterson, G. Le, V. Angelopoulous, G. D. Reeves, M. B. Moldwin, and F. K. Chun, Plasmaspheric depletion and refilling associated with the September 25, 1998 magnetic storm observed by ground magnetometers at *L*=2, *Geophys. Res., Lett., 27*, 633-636, 2000.

Cooper, M. L., C. R. Clauer, B. A. Emery, A. O. Richmond, and J. D. Winningham, A storm time assimilative mapping of ionospheric electrodynamics analysis for the severe geomagnetic storm of November 8-9, 1991, *J. Geophys. Res., 100*, 19,329-19,342, 1995.

Fedder, J. A., and J. G. Lyon, The solar wind-magnetosphere-ionosphere current-voltage relationship, *Geophys. Res. Lett., 14*, 880-883, 1987.

Mulligan, T., C. T. Russell, and J. G. Luhmann, Solar cycle evolution of the structure of magnetic clouds in the inner heliosphere, *Geophys. Res. Lett., 25*, 2959-2962, 1998.

Raeder, J., J. Berchem, and M. Ashour-Abdalla, The Geospace Environment Modeling Grand Challenge: Results from a global geospace circulation model, *J. Geophys. Res., 103*, 14,787-14,797, 1998.

Reiff, P. H., and J. G. Luhmann, Solar wind control of the polar cap potential, in *Solar Wind-Magnetosphere Coupling*, edited by Y. Kamide and J. Slavin, pp 453-476, Terra Sci., Tokyo, 1986.

Richmond, A. D., and Y. Kamide, Mapping electrodynamic features of the high-latitude ionosphere from localized observations: Technique, *J. Geophys. Res., 93*, 5741-5759, 1988.

Ridley, A. J., G. Lu, C. R. Clauer, and V. D. Papitashvili, A statistical study of the ionospheric convection response to changing interplanetary magnetic field conditions using the assimilative mapping of ionospheric electrodynamics technique, *J. Geophys. Res., 103*, 4023-4039, 1998.

Scurry, L., and C. T. Russell, Proxy studies of energy transfer in the magnetosphere, *J. Geophys. Res., 96*, 9541-9548, 1991.

Weimer, D. R., Models of high-latitude electric potentials derived with a least error fit of spherical coefficients, *J. Geophys. Res., 100*, 19,595-19,607, 1995.

Weimer, D. R., An improved model of ionospheric electric potentials including substorm perturbations and application to Geospace Environment Modeling November 24, 1996 event, *J. Geophys. Res., 106*, 407-416, 2001.

G. Lu, High-Altitude Observatory, NCAR, P.O. Box 3000, Boulder, CO 80307.

J. G. Luhmann, Space Sciences Laboratory, University of California, Berkeley, CA 94720.

C. T. Russell, Institute of Geophysics and Planetary Physics, University of California, 3845 Slichter Hall, 405 Hilgard Avenue, Los Angeles, CA 90095-1567. (ctrussell@igpp.ucla.edu)

(Received August 9, 2000; revised February 16, 2001;
accepted April 10, 2001.)